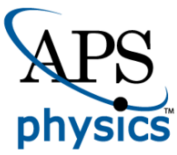

Realization of a Floquet-Engineered Moat Band for Ultracold Atoms

C. A. Bracamontes, J. Maslek, and J. V. Porto

Phys. Rev. Lett. **128**, 213401 — Published 24 May 2022

DOI: 10.1103/PhysRevLett.128.213401

Realization of a Floquet-engineered moat band for ultracold atoms

C. A. Bracamontes, J. Maslek and J. V. Porto
Joint Quantum Institute,
University of Maryland and National Institute of Standards and Technology,
College Park, MD 20742, United States of America

(Dated: April 14, 2022)

We experimentally engineer a moat-like dispersion in a system of weakly interacting bosons. By periodically modulating the amplitude of a checkerboard optical lattice, the two lowest isolated bands are hybridized such that the single particle energy displays a continuum of nearly degenerate minima that lie along a circle in reciprocal space. The moat-like structure is confirmed by observing a zero group velocity at nonzero quasimomentum and we directly observe the effect of the modified dispersion on the trajectory of the center of mass position of the condensate. We measure the lifetime of condensates loaded into different moat bands at different quasimomenta and compare to theoretical predictions based on a linear stability analysis of Bogoliubov excitations. We find that the condensate decay increases rapidly as the quasimomentum is decreased below the radius of the moat minimum, and argue that such dynamical instability is characteristic of moat-like dispersions, including spin-orbit coupled systems. The ground state of strongly interacting bosons in such degenerate energy landscapes is expected to be highly correlated, and our work represents a step toward realizing fractional quantum Hall-like states of bosons in an optical lattice.

The ground state of systems whose low energy single-particle states have a continuous degeneracy are typically strongly correlated and exhibit novel behavior [1–4]. There is significant interest in engineering such continuous ground state degeneracy, one of the simplest cases being a moat-like dispersion, with a continuum of degenerate minima that lie along a closed loop in reciprocal space. The determination of the interacting many-body ground state for this simple 1D degeneracy, remains an interesting problem [5–12]. Even in the weakly interacting, mean field limit, where strong correlations are not expected, the nature of the low energy states is unclear. For non-interacting bosons in 3D with a moat dispersion, the density of states is two-dimensional at low energy, and Bose-Einstein condensation (BEC) at finite temperature is not expected. Interactions play an important role in the condensate stability, however, and BEC at finite temperature has been predicted for the interacting system [13, 14].

Proposed approaches to produce moat-like energy dispersions include inducing Rashba spin-orbit coupling (SOC) [15] and Floquet engineering the desired band in a driven optical lattice [11]. In both cases, the modified dispersion results from hybridizing different motional states. Experimentally, approximate moat-like dispersions have been realized with ultracold atoms using SOC [15–18]. The resulting dispersions retain the discrete rotational symmetry of the spin-orbit coupling beams, and the moat minimum consists of 3 or 4 distinct minima instead of a completely degenerate ring [20].

In this work, we employ a Floquet engineering approach to realize a system of interacting bosons with a moat-like dispersion, similar to the proposal in Ref. [11]. The technique does not rely on having a specific atomic species with a particular spin structure, and can hence be applied to a range of bosonic and fermionic systems.

Using an optical lattice consisting of a two-dimensional checkerboard array of one-dimensional tubes, we hybridize [21] its two lowest energy bands [Fig. 1(a)] by

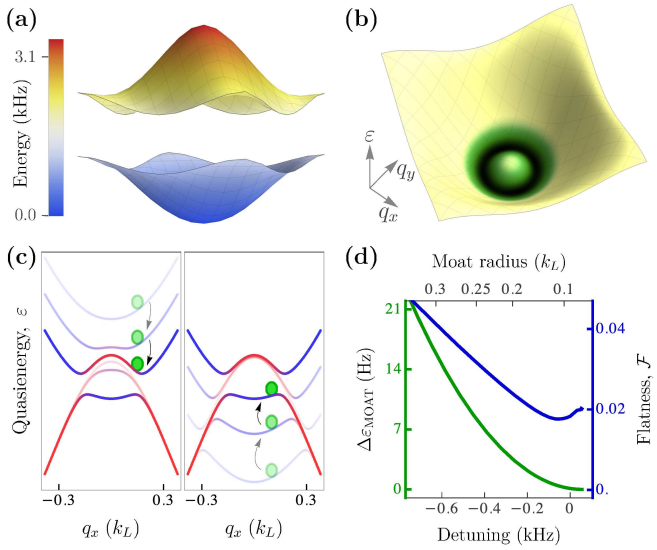

FIG. 1. Generation of a moat band via amplitude modulation. (a) Lowest bare energy bands of the checkerboard lattice, plotted versus quasimomentum $\vec{q} = (q_x, q_y)$ over the first Brillouin zone. (b) Floquet-Bloch band with nearly degenerate moat-like minima, resulting from hybridization of the bands in (a). (c) Cross section along $q_y = 0$ of the quasienergy spectrum $\varepsilon(\vec{q})$ showing both dressed bands. Left: adiabatic preparation of a condensate, initially occupying the bare ground band, into the upper band by sweeping the drive frequency down, starting above resonance. Right: preparation into the lower band by sweeping the frequency up. (d) Peak-to-peak variation of ε along the moat, $\Delta\varepsilon_{\rm MOAT}$, and moat flatness $\mathcal{F}$ versus detuning of the drive. The moat radii are indicated in the upper axis.

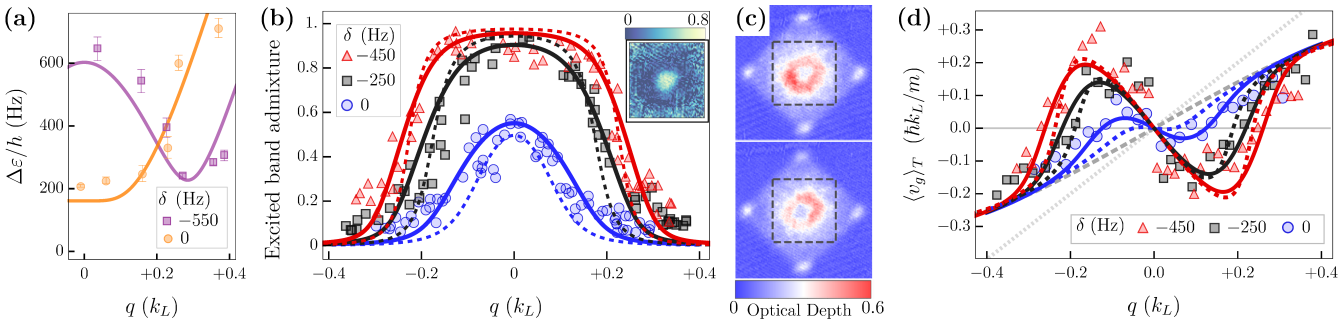

FIG. 2. Dressed band spacing, bare band admixture and group velocity profiles of the Floquet bands as a function of quasimomentum q, measured along a line passing through the center of the Brillouin zone (BZ1). (a) Spacing $\Delta\varepsilon$ between the Floquet bands at two detunings, as measured from quench dynamics. Solid lines indicate calculated spacings. (For $\delta = -550$ Hz only, $\alpha_m = 0.18$.) (b) Measured bare excited band admixture for Floquet states in the moat band. The solid (dashed) lines are the admixture calculated with (without) mean-field interactions. Marker shapes correspond to different modulation detunings. The inset shows an example of a single-shot two-dimensional admixture profile within BZ1, calculated from absorption images of heated clouds like those shown in (c), where dashed lines outline BZ1. (d) Time-averaged group velocity $\langle v_g \rangle_T$ for Floquet states in the moat band. The solid and dashed colored lines are calculated numerically assuming interacting and non-interacting particles, respectively (see [19]). The dashed (dotted) gray line indicates the group velocity associated with the bare lattice (free-particle) dispersion.

modulating the lattice depth. The form of the resulting dressed bands $\varepsilon_i(\vec{q})$ depends on the frequency f_m and fractional amplitude α_m of the modulation [Fig. 1(c)]. (Unless otherwise noted, $\alpha_m = 0.12$.) For drive frequencies near the bare band gap, one of the hybrid bands (which we denote the "upper" band) has a nearly circular minimum at nonzero radius $q_{\min}$ [Fig. 1(b)].

Our method is expected to possess a high intrinsic rotational symmetry, allowing for smaller absolute energy variation along the moat minimum than typical Raman coupled SOC schemes [15–18]. Figure 1(d) presents two measures of the moat degeneracy calculated as a function of the detuning of f_m relative to the $\vec{q} = 0$ bare band gap. The magnitude of the peak-to-peak amplitude of ε along the moat, $\Delta\varepsilon_{\mathrm{MOAT}}$, is less than 21 Hz over the entire range. The predicted flatness $\mathcal{F}$, defined as the ratio of $\Delta\varepsilon_{\mathrm{MOAT}}$ relative to the local maximum of the band at $\vec{q} = 0$, is similar to the flatness determined in Ref. [11].

Our experiment begins with a ^{87}Rb BEC in the $|F = 1, m_F = -1\rangle$ state held in a hybrid trap, consisting of a crossed optical dipole trap and a vertically offset magnetic quadrupole trap. A 2D checkerboard lattice [22, 23] with $\lambda = 813$ nm is adiabatically loaded in 200 ms to a depth $V_0 = 5.9(1)\, E_R$, with a staggered offset $0.44(1)\, E_R$ between neighboring sites (here, $E_R = \hbar^2 k_L^2/2m = h\times 3.5$ kHz is the single-photon recoil energy, $k_L = 2\pi/\lambda$ is the single-photon wave-vector and m is the mass of ^{87}Rb). See [19] for details. This results in the two lowest bare bands having a spacing at $\vec{q} = 0$ of $h\Delta_0 = h\times 3.2$ kHz, both separated from the next nearest (weakly-coupled) excited band by at least $h\times 5.2$ kHz. In the presence of the lattice, the trap frequencies are $\omega_\perp/2\pi = 11(1)$ Hz, $\omega_z/2\pi = 50(2)$ Hz, and the atomic cloud (containing approximately 10^4 atoms) possesses an average mean-field interaction energy on the order of $h\times 125$ Hz, which drops to $h\times 70$ Hz in the absence of the lattice.

We first demonstrate the effectiveness of amplitude modulation to hybridize the lowest bare bands by measuring the spacing between the dressed bands $\Delta\varepsilon(\vec{q})$ for two different detunings, $\delta = f_m - \Delta_0$. To extract the values of $\Delta\varepsilon$, shown in Fig. 2(a), we observe the bare band population dynamics after a sudden quench into the dressed bands [19, 24]. To observe the dynamics, we measure the relative populations after a band map [25], where the lattice is ramped off in 800 µs. For measurements at nonzero quasimomenta, a kick is imparted to the condensate before the modulation starts, by suddenly translating the magnetic quadrupole field. This induces oscillatory motion of the cloud along a line passing through the center of the trap in the unmodulated lattice. For detuning $\delta = -550$ Hz, the measured dressed band spacing has a minimum $\simeq 200$ Hz ($0.06\ E_R/h$) at $q \simeq 0.3\, k_L$, as expected from calculations.

In order to adiabatically prepare the condensate in a single dressed band, the amplitude modulation coupling the two bands is slowly turned on, starting off-resonance. The magnitude and frequency of the coupling are simultaneously ramped to their final values in 12 ms starting at a detuning $|\delta| > 600$ Hz [19]. The direction of the frequency sweep determines which dressed band the BEC is loaded into: a sweep starting blue (red) detuned and ending close to resonance prepares atoms in the upper (lower) dressed band [see Fig. 1(c)].

We measure the bare band admixture of the experimentally prepared state immediately after the 12 ms ramp as a function of $\vec{q}$ and compare it to the expected bare state populations, see Fig. 2(b). The theoretical profiles from a non-interacting Floquet calculation [Fig. 2(b), dashed lines] capture the magnitude of the admixture, particularly near the center of the band. A nonlinear mean-field calculation based on the time-dependent

Gross-Pitaevskii equation [19] improves the overall agreement with the data [Fig. 2(b), solid lines]. The inset shows an example of the 2D bare band admixture measured with a heated cloud having a significant spread around the center of the first Brillouin zone (BZ1), showing the 2D nature of the moat band. The admixture is more azimuthally homogeneous than the raw populations [Fig. 2(c)], whose distribution is affected by both stochastic and systematic fluctuations of the initial momentum of the BEC.

The dispersion $\varepsilon(\vec{q})$ determines the condensate's center of mass velocity v_g, which is related to the gradient of the Floquet band according to $\nabla_{\vec{q}}\varepsilon = \hbar\langle v_g\rangle_T$, where $\langle\ldots\rangle_T$ indicates time-average over a single period $T = 1/f_m$ of the modulation [26–28].

We measured v_g under the same conditions used for the admixture profile [Fig. 2(b)], except that the bare band population detection was replaced by a diabatic snap-off of the lattice, which projects the condensate onto its plane-wave components. Micromotion during the drive period gives rise to periodic instantaneous v_g, which we account for by averaging over different snap-off times relative to T. The values of v_g were extracted from time-of-flight (TOF) images by computing the mean velocity of the momentum peaks, weighted by their populations. The measured $\langle v_g\rangle_T$ profile, presented in Fig. 2(d), is the result of averaging v_g at modulation phases 0, $\pi/2$ and π, corresponding to maximum, average and minimum lattice intensities. A vanishing group velocity for nonzero $\vec{q}$, a feature easily recognized in the black and red data, is a clear signature of a band with a moat-like shape.

Spectroscopic measurements like those in Fig. 2 provide information about dressed energies, but do not capture the modified dressed state behavior. While the data in Fig. 2(d) directly show the velocity, it is an instantaneous measurement. The modification of v_g should impact the motional dynamics of the BEC in the trap, if the heating of the BEC is sufficiently small relative to the timescale of the trap.

Figure 3 shows the expected and observed motional dynamics of the BEC in the trap after adiabatic preparation in the upper dressed state with an initial $\vec{q} \neq 0$ for bands with different moat radii. Theoretical calculations of the time evolution of $\vec{q}$, superimposed on the corresponding dispersion, are presented in Fig. 3(a). These trajectories were computed using quasiclassical equations of motion [29]: $d\vec{q}/dt = \hbar^{-1} f_{\rm trap}(\vec{r}_c)$, $d\vec{r}_c/dt = \hbar^{-1}\nabla_{\vec{q}}\varepsilon$, where $f_{\rm trap}$ is the force exerted by the harmonic trap, $\vec{r}_c$ is the condensate's position, and ε is the quasienergy spectrum inferred from the calibration of lattice parameters. Initial conditions $(\vec{q}_0, \vec{r}_{c0})$ are the same for all curves, and were chosen so that the trajectories have a significant dependence on the moat position. For the unmodulated case, the trajectory is a standard ellipse associated with the isotropic harmonic trap. For the modulated case, the change in effective mass significantly modifies the atoms' response to the restoring force of the trap.

We experimentally verified the effect of the dressed band dispersion on the dynamics of a condensate. Using parameters that produce the effective bands in Fig. 3(a), we measured the position after time-of-flight as a function of the time held in the moat band [see Fig. 3(b)], using a two-kick sequence that results in elliptical motion for the unmodulated case. (The scaled time-of-flight position is approximately equal to $\vec{q}/k_L$, with a small additional contribution from the position $\vec{r}_c$, see [19].) Although heating effects limited the longest hold time in the dressed band to 26 ms (black curve) and 21 ms (red curve), the effect of the modification of the dispersion on the motion in the trap is evident.

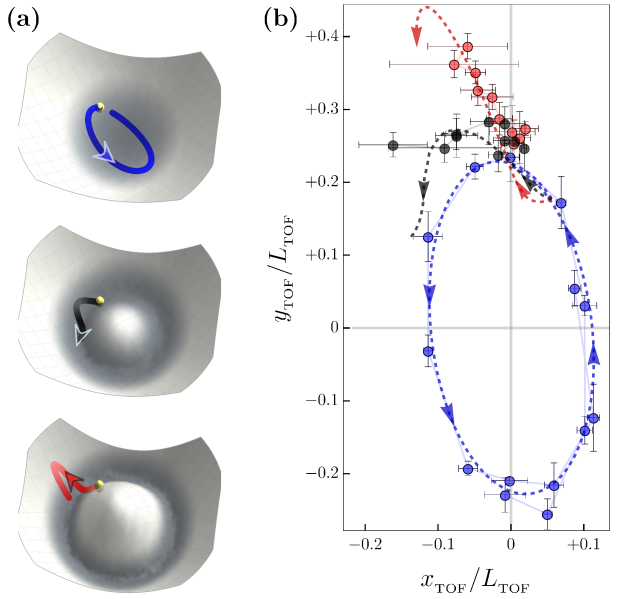

FIG. 3. Time evolution of quasimomentum in different moat bands for the same initial conditions. (a) Predicted quasimomentum trajectories, plotted on top of the respective quasienergy spectrum. Yellow dots indicate the initial value of $\vec{q}$. Blue, black and red curves correspond to moats with radii 0 k_L (no modulation), 0.23 k_L and 0.30 k_L. (b) Position after time-of-flight, $(x_{\rm TOF}, y_{\rm TOF})$, scaled by $L_{\rm TOF} = \hbar k_L/mT_{\rm TOF}$, for different times held in the effective moat band. Experimental data taken under conditions that yield dressed bands similar to those shown in (a). Blue points were obtained in the absence of modulation. Modulation frequencies for the black and red points are $f_m = 2.90$ kHz and $f_m = 2.65$ kHz, respectively. Time elapsed for blue, black and red points is 130 ms, 26 ms and 21 ms, respectively. Dashed lines are the predicted position after time-of-flight for condensates held in the bands shown in (a).

Instabilities and heating are known to hamper the realization of effective Hamiltonians using Floquet engineering [30]. We examined the heating that limits the lifetime of condensed dressed states in both Floquet bands. Figure 4(a) shows the measured condensate fraction decay rates for BECs loaded into the upper and lower hybridized band as a function of the detuning δ, which changes the moat radius $q_{\rm min}$ of the upper band. Rates were measured for condensates prepared at $|\vec{q}| = 0\,k_L$

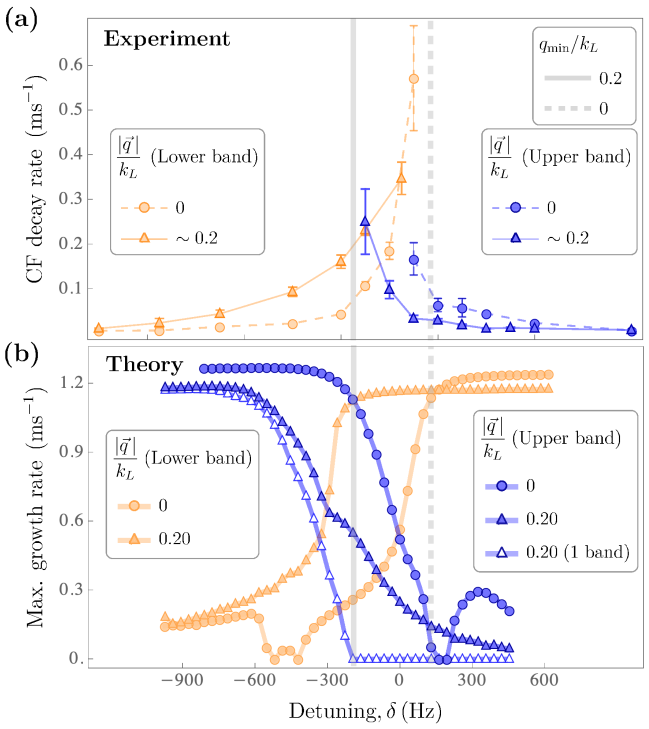

FIG. 4. Instabilities of a condensate in the dressed bands. (a) Observed condensate fraction decay rates for BECs in lower and upper bands. For each band, we measured rates for $|\vec{q}| = 0\,k_L$ and $|\vec{q}| \simeq 0.2\,k_L$. The solid (dashed) vertical gray line indicates the frequency at which the moat radius $q_{\min}$ is $0.2\,k_L$ ($0\,k_L$). (b) Calculation of the growth rate of the most unstable mode, based on a Floquet-Bogoliubov linear stability analysis for conditions similar to those in (a). The instability rate calculated for $|\vec{q}| = 0.2\,k_L$ including only contributions from the single BEC-occupied band are shown with open symbols. The unoccupied band induces increased decay for $|\vec{q}|$ near resonance.

and $|\vec{q}| \simeq 0.20\,k_L$. To keep an approximately constant value of $|\vec{q}|$ during the decay measurement, we carefully prepare the initial condition so that the resulting trajectory is circular. We find that the decay rates in the upper band increase dramatically when $|\vec{q}|$ approaches $q_{\min}$, becoming difficult to measure for $|\vec{q}| < q_{\min}$.

To understand the condensate decay, we modeled the system with a periodically driven Gross-Pitaevskii equation and calculated condensate depletion rates using a linear stability analysis similar to the technique in Refs. [31, 32] (see [19]). In Figure 4(b) we present the theoretical condensate depletion rates, which are calculated as the largest growth rate of the unstable modes, for the frequency range used for the data in Fig. 4(a). The frequencies at which the condensate in the upper and lower bands are most unstable differ substantially, due to the opposite band curvatures [33]. We find that there are two contributions to the decay: intra-band scattering processes within the dressed band and inter-band scattering between the bands. The intra-band processes are fundamentally related to the shape of the band, and dynamical instabilities [34, 35] for a moat-like dispersion generally arise for $|\vec{q}| < q_{\min}$, where the band curvature becomes negative along the direction perpendicular to $\vec{q}$. On the other hand, the inter-band processes are not restricted to $|\vec{q}| \gtrsim q_{\min}$. Figure 4(b) (open triangles) shows the stability analysis restricted to the single moat band, and it shows no decay until the sudden turn on of loss at $|\vec{q}| = q_{\min}$. Despite the fact that the mode stability analysis is only applicable to the initial exponential dynamics that are dominated by decay into a single mode, the model captures the overall scale of the condensate decay rate and its dependence on detuning.

Previous theoretical work [13, 14] in the Rashba SOC system with similar moat-like dispersion indicates that a single-momentum condensate is stable exactly at $|\vec{q}| = q_{\min}$. This is consistent with the absence of inter-band processes contributing to the decay for $|\vec{q}| \geq q_{\min}$ for the Rashba case. However, while the stability analysis shows that the condensate is stable at the moat minima, we note that, as with our case, the Rashba SOC system is also unstable for $|\vec{q}| < q_{\min}$, and therefore sits at a critical point in momentum space [19, 36]. The $|\vec{q}| < q_{\min}$ instability is related to the curvature of the moat band, and is generally present, regardless of the underlying mechanism for generating the moat. It is indicative of the fact that the BEC is not a many-body eigenstate of the static effective Halmiltonian. The fact that the moat minima coincide with the boundary of the instability region likely has implications for the ground state of the system, even in the weakly-interacting limit. The $|\vec{q}| \gtrsim q_{\min}$ instability is due to resonant coupling to the second band and depends on the specific lattice configuration used. It can be avoided under configurations lacking resonant dispersion conditions [19].

The instability at $|\vec{q}| < q_{\min}$ can be seen in Figure 4(b) where we show the single-band linear stability analysis calculation (open triangles). The decay rate increases sharply from near-zero at $|\vec{q}| = q_{\min}$. The contribution from the lower band induces more loss in the region $|\vec{q}| \gtrsim q_{\min}$, as shown by the two-band calculation (blue filled triangles).

In conclusion, we have engineered a moat-like dispersion for ultracold atoms in an optical lattice, and confirmed the dispersion by measuring the dynamics of a BEC in the modulated lattice. We measured condensate lifetimes under various moat conditions. Besides the condensate decay inherent to the moat band shape, our model suggests that interactions coupling to the other dressed band can be significant and need to be considered in systems involving near resonant hybridization.

The many-body ground state of interacting bosons in the low density, strongly correlated limit in such a moat remains an open question [5–11]. It has been argued [8–11] that the low density ground state in a moat-like dispersion is a composite-fermion-like state leading to a chiral spin liquid, and it will be interesting to explore this limit experimentally. Reaching the highly correlated

regime requires confinement in the transverse direction (attainable with the addition of an out-of-plane optical lattice) to ensure the system is fully 2D. Additionally, the density would need to be much lower; for example, with $q_{\min} \lesssim 0.3\,k_{\mathrm{L}}$, the density should not exceed one atom per ten lattice sites [11]. It remains an outstanding experimental and theoretical question as to how to prepare a low energy state in such a system, as well as how and how quickly the correlated system heats.

We acknowledge stimulating conversations with Victor Galitski and Ian Spielman.

[1] H. L. Stormer, D. C. Tsui, and A. C. Gossard, Rev. Mod. Phys. **71**, S298 (1999).
[2] S. D. Huberand E. Altman, Phys. Rev. B **82**, 184502 (2010).
[3] D. Leykam, A. Andreanov, and S. Flach, Advances in Physics: X **3**, 1473052 (2018).
[4] V. Galitskiand I. B. Spielman, Nature **494**, 49 (2013).
[5] S. Gopalakrishnan, A. Lamacraft, and P. M. Goldbart, Phys. Rev. A **84**, 061604 (2011).
[6] Q. Zhouand X. Cui, Phys. Rev. Lett. **110**, 140407 (2013).
[7] S. Surand K. Yang, Phys. Rev. B **100**, 024519 (2019).
[8] T. A. Sedrakyan, A. Kamenev, and L. I. Glazman, Phys. Rev. A **86**, 063639 (2012).
[9] T. A. Sedrakyan, L. I. Glazman, and A. Kamenev, Phys. Rev. B **89**, 201112 (2014).
[10] T. A. Sedrakyan, L. I. Glazman, and A. Kamenev, Phys. Rev. Lett. **114**, 037203 (2015).
[11] T. A. Sedrakyan, V. M. Galitski, and A. Kamenev, Phys. Rev. Lett. **115**, 195301 (2015).
[12] H. Zhai, Reports on Progress in Physics **78**, 026001 (2015).
[13] T. Ozawaand G. Baym, Phys. Rev. Lett. **109**, 025301 (2012).
[14] R. Barnett, S. Powell, T. Graß, M. Lewenstein, and S. Das Sarma, Phys. Rev. A **85**, 023615 (2012).
[15] D. L. Campbell, G. Juzeliūnas, and I. B. Spielman, Phys. Rev. A **84**, 025602 (2011).
[16] L. Huang, Z. Meng, P. Wang, P. Peng, S.-L. Zhang, L. Chen, D. Li, Q. Zhou, and J. Zhang, Nature Physics **12**, 540 (2016).
[17] J. Hou, H. Hu, K. Sun, and C. Zhang, Phys. Rev. Lett. **120**, 060407 (2018).
[18] A. Valdés-Curiel, D. Trypogeorgos, Q. Y. Liang, R. P. Anderson, and I. B. Spielman, Nature Communications **12**, 593 (2021).
[19] See Supplemental Material at *** for additional information.
[20] S. Zhangand G.-B. Jo, *Spin-Orbit Coupled Materials*, Journal of Physics and Chemistry of Solids **128**, 75 (2019).
[21] C. V. Parker, L.-C. Ha, and C. Chin, Nature Physics **9**, 769 (2013).
[22] J. Sebby-Strabley, M. Anderlini, P. S. Jessen, and J. V. Porto, Phys. Rev. A **73**, 033605 (2006).
[23] S. B. Koller, E. A. Goldschmidt, R. C. Brown, R. Wyllie, R. M. Wilson, and J. V. Porto, Phys. Rev. A **94**, 063634 (2016).
[24] A. Valdés-Curiel, D. Trypogeorgos, E. E. Marshall, and I. B. Spielman, New Journal of Physics **19**, 033025 (2017).
[25] J. H. Denschlag, J. E. Simsarian, H. Häffner, C. McKenzie, A. Browaeys, D. Cho, K. Helmerson, S. L. Rolston, and W. D. Phillips, Journal of Physics B: Atomic, Molecular and Optical Physics **35**, 3095 (2002).
[26] S. Arlinghausand M. Holthaus, Phys. Rev. B **84**, 054301 (2011).
[27] While the time average of an observable over micromotion does not in general equal the Floquet effective quantity, the time average in the equation $\nabla_{\bar{q}}\varepsilon = \hbar\langle v_g\rangle_T$ is correct for v_g, see Ref. [26].
[28] A generalization of the equation $\nabla_{\bar{q}}\varepsilon = \hbar\langle v_g\rangle_T$ to a nonlinear mean-field context, where the wave function of the condensate is described by the time-dependent Gross-Pitaevskii equation, is given in the Supplemental Material [19].
[29] A. R. Kolovskyand H. J. Korsch, Phys. Rev. A **67**, 063601 (2003).
[30] A. Eckardt, Rev. Mod. Phys. **89**, 011004 (2017).
[31] M. Modugno, C. Tozzo, and F. Dalfovo, Phys. Rev. A **70**, 043625 (2004).
[32] S. Lellouch, M. Bukov, E. Demler, and N. Goldman, Phys. Rev. X **7**, 021015 (2017).
[33] B. Wuand Q. Niu, New Journal of Physics **5**, 104 (2003).
[34] B. Wuand Q. Niu, Phys. Rev. A **64**, 061603 (2001).
[35] L. Fallani, L. De Sarlo, J. E. Lye, M. Modugno, R. Saers, C. Fort, and M. Inguscio, Phys. Rev. Lett. **93**, 140406 (2004).
[36] Q. Zhu, C. Zhang, and B. Wu, Eur. Phys. Lett. **100**, 50003 (2012).